City Research Online

City, University of London Institutional Repository

This is the accepted version of the paper.

This version of the publication may differ from the final published version.

New Constitutive Relations for RC Elements Strengthened with FRP Sheets

by

Yashar Moslehy[1], Moheb Labib[2], and Ashraf Ayoub[3]

[1] Principal Technical Professional, Energo Eng. (A KBR Company), Houston, TX, USA
[2] Senior Technical Professional, KBR Inc., Houston, TX, USA
[3] Prof. of Civil Eng., City University London, London, UK

Abstract

Fiber-reinforced Polymer (FRP) started to find its way as an economical alternative material in civil engineering during the early 1970s. The behavior and failure modes for FRP composite structures were studied through extensive experimental and analytical investigations. While research related to the flexural behavior of FRP-strengthened elements has reached a mature phase, studies related to FRP shear strengthening is still in a less advanced stage. In all proposed models to predict the shear capacity, the constitutive behavior of concrete and FRP was described independently. The true behavior, however, should account for the high level of interaction between the two materials. Constitutive relations for FRP-strengthened reinforced concrete elements should provide a better understanding of the shear behavior of the composite structure. In order to generate these relations, large-scale tests of a series of FRP-strengthened reinforced concrete panel elements subjected to pure shear are conducted. The University of Houston is equipped with a unique universal panel testing machine that was used for this purpose. The paper presents the results of the test program and the calibration of the parameters of the constitutive model. These new constitutive laws could be easily implemented into finite element models to predict the behavior of externally bonded FRP strengthened beams.

Introduction

The shear design and behavior of typical reinforced concrete structures has been extensively studied in the past several decades. Such design requires knowledge of the constitutive behavior of reinforced concrete elements subjected to a biaxial state of stress. These constitutive models were accurately derived from experimental test data on representative reinforced concrete panel elements. Also, the complex behavior and failure modes of FRP composite structures were studied through extensive experimental and analytical investigations. While research related to the flexural behavior of FRP-strengthened elements has reached a mature phase, studies related to FRP shear strengthening is still in a less advanced stage. In all proposed models to predict the shear capacity, the constitutive behavior of concrete and FRP was described independently. The true behavior, however, should account for the high level of interaction between the two materials. There is an obvious need to evaluate the constitutive laws of reinforced concrete elements retrofitted with FRP sheets under pure shear.

Fiber reinforced polymer (FRP) strengthened members are typically modeled with two-dimensional continuum elements. Such models can accurately describe the behavior of the beam elements. With the inclusion of shear deformations and proper concrete constitutive models under a biaxial state of stress, fiber-based beam finite element models can also accurately simulate the behavior of FRP- strengthened girders. The objective of this work is to develop accurate constitute material laws for FRP shear-strengthened RC girders suitable for inclusion in finite element models. The University of Houston is equipped with a unique universal panel testing machine that was used for this purpose. This universal panel tester is the only one of its kind in the United States, and one of only two in the world that allows for both displacement and force-controlled load application through its newly upgraded servo-control system. The results of

the panel tests are needed to improve the basic understanding of the complex constitutive behavior of the concrete element and its interaction with the composite material, which will help to provide a proper description of analytical models. A review of previous studies in the field is presented first.

REVIEW OF PREVIOUS RESEARCH STUDIES

The current literature documents a variety of work related to the behavior of RC structures retrofitted by FRP sheets. Although the first research projects on FRP material started in the 80s, the first analytical model came out by Triantafillou (1998). After that, many researchers tried to expand the subject by performing experimental tests and analytical work. Triantafillou and Antonopoulos (2000) tried to improve their model. Khalifa et al. (1998, 1999), Pellegrino and Modena (2002), Chaallal et al. (1998, 2002), Hsu et al. (2003), Zhang and Hsu (2005) and Deniaud and Cheng (2004) developed models based on effective FRP strains as a function of the FRP stiffness, or based on bond mechanism. Another group of researchers including Chen and Teng (2003a-b), Monti and Liotta (2005), Cao et al. (2005) and Carolin and Taljsten (2005) came up with models based on non-uniform strain distributions. The American concrete institute (ACI) in 2002 published the ACI440.2R-02 (2002) guidelines which were backed by the idea of design based on effective FRP strain as function of FRP stiffness or based on bond mechanism. Tumialan (2007) performed an extensive study on all the existing models for predicting the behavior of RC beams retrofitted by FRP sheets and found out that none of the analytical models and design guidelines/codes/specifications was able to provide reliable estimates; which indicates that the mechanisms of FRP strengthening for shear are still poorly understood. As a result, parameters that are not taken into account in these analytical and design methodologies, but that affect the behavior of members strengthened in shear with FRP, were identified. Several finite element models for FRP-strengthened concrete structures were also developed. Through

the research of the co-authors, fiber beam elements have proven to be able to model the behavior of beams and walls rather well, and are computationally very efficient (Lu and Ayoub, 2011). With the inclusion of shear deformations and proper concrete constitutive models under a biaxial state of stress, fiber models can also accurately simulate the behavior of FRP-strengthened beams (Mullapudi and Ayoub, 2010).

This brief background shows the obvious need to a deeper study on all aspects of RC structures strengthened with FRP for shear, which is impossible without evaluating the proper constitutive relation of its behavior. This study represents the first step of reaching this goal, which is trying to evaluate the constitutive behavior of cracked concrete retrofitted by FRP sheets using panel tests of representative elements.

THE UNIVERSAL PANEL TESTER

The universal panel tester (UPT) used to conduct the study was constructed at the University of Houston in 1986 (Hsu et al. 1995), and is shown in Fig. 1. The largest size of a reinforced concrete panel that can be tested is 55 x 55 in. (1400 x 1400 mm), with a thickness up to 16 in. (406 mm). The panel tester houses 40 in-plane hydraulic cylinders that are used to apply in-plane membrane forces on full-scale reinforced concrete panels. The width of the panel is spanning in the west and east directions. One side of the panel is facing the north direction, and the other side is facing the south direction. Since the construction of the panel tester, a steel frame was prepared and installed on the machine to facilitate mounting of additional 20 out-of-plane cylinders. To achieve equilibrium, out of the 40 in-plane cylinders, there were three rigid links located on the north face of the panel. Two of these rigid links were at the top line of the panel, and the third was at the right side of it. Similarly, there were three rigid links in the out-of-plane direction. The purpose of the rigid links was to provide stability for the specimens and to resist

4

any unequal forces acting on the specimen due to friction or any other reason. The maximum possible operating hydraulic pressure for the pump used to load the hydraulic cylinders is 5000 psi (34.5 MPa).

The control in the movement of the cylinders can be performed manually or automatically. The manual control is used when installing the specimens, while the automatic control is typically used when testing the specimens. Originally, the automatic control used to allow for testing under load control only, but in 1995, a servo-control system was installed so that strain-controlled tests could be also performed. The servo-control system is prepared with 10 servo controllers which in turn are connected to 10 hydraulic manifolds. Each manifold is divided internally into two chambers, with a servo valve in each manifold to determine how much pressure will flow in each chamber. Outside of each manifold, there are two columns of 10 quick connect-disconnect connectors. Each group of the 40 in-plane or the 20 out-of-plane cylinders that are required to apply the same load is connected to the same manifold. There is a pressure transducer on the bottom of each manifold that measures the pressure in each chamber and reports it back to the servo controller. The servo controller takes the command from the computer or the programmer and sends orders to the servo valve. At the same time, the servo controller receives feedback from the pressure transducer and modifies its orders to the servo valve to reduce the error between the feedback and the command. The servo controller can take the command from the computer, the rigid links, or the readings from instrumentations on the surface of the panel in the case of strain-controlled tests. Figures 1 and 2 show the universal panel tester with a tested panel inside it.

TEST PROGRAM

This section presents the details of the construction and testing of twelve specimens that were subsequently tested under the effect of sequential in-plane shear stresses. In addition to application of two different FRP reinforcement thicknesses, these twelve specimens were subjected to a varying amount of tensile strain, before an in-plane compressive load was applied until failure. Out of these twelve specimens only eight could be successfully tested and the rest were unsuccessful due to several reasons which will be shortly discussed in this paper. These panels were reinforced with two layers of No. 4 steel reinforcement grids, which is equivalent to a reinforcement ratio of 0.0067 in both directions, but with two different detailing which are shown in Figure 3 as configurations A and B. The reinforcement ratio in each direction was calculated based on the steel bars within the instrumented region. The results of these eight specimens were compared with a similar control specimen tested by Belarbi and Hsu (1994, 1995) under the same type of loading. The control panels were made of plain RC panels, with the only difference being in the strengthening with FRP strips on the surface of the panels. These external reinforcements were used with different wrapping schemes (Figure 4) in order to find the most efficient and applicable one. The specimens that were subjected to sequential loads were noted Specimens F1P-1 to F1P-8 and F2P-1 to F2P-4. The letter F refers to FRP, numbers 1 or 2 after it define the FRP type (Tyfo SCH11-UP with thickness of 0.27 mm or Tyfo® SCH-41S with thickness of 1 mm from Fyfe co., respectively) that was used. The number afterward refers to the number of the tested panel. Either "N" or "S" was added to the panel name to distinguish between the results of the north and south sides of the panel respectively.

The specimens were all 55 in. (1400 mm) square with a thickness of 7 in. (178 mm). The reinforcement bars were aligned at an angle of 90 degrees, as shown in Figure 3. The

reinforcement bars were spanning from one end of the panel to the other, and were welded to steel inserts at the edges of the panel. Welding the reinforcement grid to the steel inserts was conducted in two stages. The first direction of the grid was welded to the inserts before aligning the inserts inside the formwork, while the second direction was welded after fixing the inserts inside the formwork. These steel inserts are typically used to connect the panel to the steel yoke of the main frame using high-strength bolts, which in turn is connected to the hydraulic cylinders using pins made of alloy steel with diameter of 3.6 in. (91 mm).

Threaded rods with length equivalent to the thickness of the specimen were fixed in the form work before placing the concrete. These rods are used to hold the instrumentations on the two faces of the panel needed to measure the developed strains. The threaded rods were distributed on the perimeter of a 31.5 in. (800 mm) square in such a way that there were four threaded rods on each side of the square. This arrangement of the threaded bars facilitate installing four vertical, four horizontal, and two diagonal linear variable differential transducers (LVDTs) on each face of the panel. Such an arrangement of the LVDTs facilitates capturing the strain across a distance of 31.5 in. (800 mm), which is the summation of the distance where the maximum tensile strains in the concrete develop in addition to the width of the developed cracks in the concrete within the measurement area.

Concrete was mixed manually using a conventional mixer in the structural lab. Due to the size of the mixer, two batches were prepared and placed in the formwork. Concrete strength of successfully tested specimens ranged between a minimum of 4030 psi (27.8 MPa) and a maximum of 6650 psi (45.8 MPa). The specimens were cured for 3 days using wet burlap and plastic sheets before being taken out of the formwork. The top surface of the panels was grinded to smooth it and to facilitate locating the cracks developed during testing. The panels were then

attached to the steel yokes. Table 1 also shows the arrangement of each tested panel with the reinforcement and FRP strips.

BEHAVIOR OF TESTED PANELS UNDER SEQUENTIAL LOADING

This section presents a discussion on the behavior of the tested specimens. All twelve panels were tested under sequential loading. The panels were first loaded in both tension and compression in the elastic region to ensure the UPT was functioning properly. The panels were then loaded in tension with an end goal of 0.0 to 0.75% tensile strain as measured by the horizontal LVDTs. Panels F1P-1, F1P-2, F1P-4 and F1P-7 had premature failure due to lack of sufficient external reinforcement and difficulties with the testing machine, respectively. For this reason only the other eight panels will be discussed in details in this section. The parameters of these panels are shown in Table 2.

Panel F1P-1 failed prematurely due to extended cracks that appeared on the panel outside the measurement area and end peeling of the FRP sheets. In attempt to prevent end peeling and to confine cracks to the measurement area, Wrapping Configuration B was considered. In this configuration, the FRP sheets extended to the edge of the panel until the area under the compressive plates. The goal was that the FRP would strengthen the whole panel equally and that the confining plates would strengthen the outside area, causing the vast majority of longitudinal strains to occur in the measurement area. Panel F1P-2 was constructed with Rebar Configuration A and Wrapping Configuration A. When testing the panel, a portion of FRP peeled off the edge of the panel, removing a mass of concrete with it. This proved catastrophic, as the panel's edge also contained the steel inserts causing two of the bottom jacks to pull their north inserts from the panel. As such, no substantial data was derived from this panel.

To fix the peeling issue, FRP Wrapping Configuration C was designed and implemented. In this configuration the FRP sheet is wrapped around the panel such that it partially overlaps the FRP sheet on the opposite side of the panel. The overlap was designed such that the panel outside of the LVDT measuring area contains two layers of FRP; while inside the measuring area has only a single layer of FRP. Additionally, to improve the inserts bond with the concrete and to prevent the rebar from failing prematurely, two shorter lengths rebars were welded to each insert. This new Rebar Configuration B, along with Wrapping Configuration B, proved to be very successful for specimen F1P-3, in which the tensile strain at failure of the panel was recorded at 0.5%. F1P-4 and F1P-6 were tested unsuccessfully due to difficulties with the testing equipment. After troubleshooting the Panel tester, panel F1P-5 crushed under compression while the tensile strain applied to the panel prior to applying compression was 0.75%. Panels F1P-7 and F1P-8 were successfully tested for 0.3% and 0% tensile strain, respectively. The second series of tests were performed using a thicker type of FRP sheet as discussed earlier, all successfully performed with tensile strains equal to 0%, 0.7%, 0.5% and 0.3% for specimens F2P-1 thru F2P-4, respectively. Figure 5 shows the crack pattern of panels after achieving the target lateral tensile strain level, while Figure 6 shows the crushing failure of panels. Figure 7 shows the crushing failure of panel F1P-5 on both sides after removing it from the panel tester. Figure 8 also shows the crushing of panel F2P-2 at failure. From these Figures, it was observed that the failure mode consisted of concrete crushing underneath the FRP sheets with no spalling to the outside because of the confinement effect of the FRP sheets.

Figure 9 shows the load-strain curves in tension for the six successful panels (which had positive target tensile strength), and confirms they have reached the proper strain target they were

9

designed for, which was held constant during the compression part of the sequential loading afterward.

STRESS SOFTENING COEFFICIENT

The peak stress-softening coefficient, ζ_σ, is defined as the ratio of peak compressive stress to the corresponding cylinder compressive strength, f_c':

$$\zeta_\sigma = \frac{\sigma_p}{f_c'} \tag{1}$$

There also exists a peak strain-softening coefficient, ζ_ε, defined as the ratio of the compressive strain at the peak panel compressive stress, ε_p, to the corresponding compressive strain at the cylinder compressive strength, ε_0:

$$\zeta_\varepsilon = \frac{\varepsilon_p}{\varepsilon_0} \tag{2}$$

However, previous studies by Belarbi and Hsu (1994, 1995) and Pang and Hsu (1995) have all found the strain-softening coefficient to be approximately equal to one. As such, this paper will focus on the stress-softening coefficient.

In the last twenty years, researchers at the University of Houston have proposed formulas to predict the stress softening coefficients of reinforced concrete (Belarbi and Hsu, 1995; Pang and Hsu, 1995, Zhang and Hsu, 1998; Wang and Hsu, 2001), prestressed reinforced concrete (Laskar et al. 2008), and steel fiber reinforced concrete (Hoffman 2010). For purposes of comparison in this paper, Wang and Hsu's work (2001) is the most relevant.

PROPOSED CONSTITUTIVE LAWS OF FRP-STRENGTHENED CONCRETE ELEMENTS

In the next sections, based on the experimental results obtained, new constitutive laws for FRP-strengthened reinforced concrete elements are proposed. These include expressions for the concrete behavior in tension, the embedded steel reinforcement in tension, the normalized concrete behavior in compression, and the stress softening coefficient of concrete. These relations can be readily used to define the constitutive behavior of elements in finite element analysis, and accounting for the interaction of concrete and FRP.

Concrete Behavior in Tension

Based on the data retrieved from the tests, considering the modulii of elasticity of steel and FRP from the material tests, and assuming that both will act elastically till the yielding strain of steel which is equal to 0.00165 in/in, the stresses in concrete up to the yielding point of steel can be evaluated. Figure 10 shows the results for specimen F1P; those of specimen F2P are identical. The concrete model in tension proposed by Belarbi et al. (1994) was deemed suitable for adoption, but the model parameters were changed to better correlate with the extracted experimental results. Based on Figure 10, the following relationships can be drawn for the behavior of concrete in tension in the presence of FRP:

<u>Ascending branch</u> $(\bar{\varepsilon}_1 \leq \varepsilon_{cr})$

$$\sigma_1^c = E_c \, \bar{\varepsilon}_1 \tag{3}$$

where

E_c = modulus of elasticity of concrete, taken as $15000\sqrt{f_c'(psi)}$, where f_c' and $\sqrt{f_c'}$ are in psi,

ε_{cr} = cracking strain of concrete, taken as 0.0002 in./in.,

Descending branch $(\bar{\varepsilon}_1 > \varepsilon_{cr})$

$$\sigma_1^c = f_{cr}\left(\frac{\varepsilon_{cr}}{\bar{\varepsilon}_1}\right)^{0.5}$$

(4)

where f_{cr} = cracking stress of concrete, taken as $3.75\sqrt{f_c'(psi)}$.

Embedded Steel Behavior in Tension

It was found based on the experimental program that the model introduced by Belarbi et al. (1994) for embedded steel reinforcement in tension is still valid for RC membrane elements strengthened with FRP strips. Figure 11 shows the results for specimen F1P for clarity; those of specimen F2P are identical. These relationships are as follow:

$$f_s = E_s \bar{\varepsilon}_s \qquad \text{when } \bar{\varepsilon}_s \le \varepsilon_y' \qquad (5)$$

$$f_s = (0.91 - 2B)f_y + (0.02 + 0.25B)E_s\bar{\varepsilon}_s \quad \text{when } \bar{\varepsilon}_s > \varepsilon_y' \qquad (6)$$

where

$$\varepsilon_y' = f_y'/E_s \qquad (7)$$

$$f_y' = (0.93 - 2B)f_y \qquad (8)$$

$$B = \frac{1}{\rho}\left(\frac{f_{cr}}{f_y}\right)^{1.5} \qquad (9)$$

Normalized Concrete Behavior in Compression – Softening Effect

Figure 12 shows the concrete stress-strain plots of all specimens normalized to $\sqrt{f_c'}$. It can be clearly seen that the higher the tensile strain, the higher the effect of softening. In addition, as the tensile strain increases, the stiffness of the panels under compressive load decreases; this decrease in stiffness is not very much dependable on the FRP thickness but mainly on the tensile strain.

12

The constitutive relationships of concrete compressive stress σ_2^c and the uniaxial compressive strain $\bar{\varepsilon}_2$ are given as follows:

$$\sigma_2^c = \zeta f_c' \left[2\left(\frac{\bar{\varepsilon}_2}{\zeta \varepsilon_0}\right) - \left(\frac{\bar{\varepsilon}_2}{\zeta \varepsilon_0}\right)^2 \right], \qquad \frac{\bar{\varepsilon}_2}{\zeta \varepsilon_0} \leq 1 \tag{10}$$

or $\quad \sigma_2^c = \zeta f_c' \left[1 - \left(\frac{\bar{\varepsilon}_2/\zeta \varepsilon_0 - 1}{4/\zeta - 1}\right)^2 \right], \qquad \frac{\bar{\varepsilon}_2}{\zeta \varepsilon_0} > 1 \tag{11}$

The softening coefficient relationship for sequential loading for plain concrete was developed as below (Wang and Hsu, 2001):

$$\zeta = \left(\frac{5.8}{\sqrt{f_c'}} \leq 0.9\right)\left(\frac{1}{\sqrt{1+250\bar{\varepsilon}_1}}\right)\left(1-\frac{|\beta|}{24°}\right) \tag{12}$$

Equation (12) consists of 3 functions:

$$\zeta = f_1(\bar{\varepsilon}_1)\, f_2(f_c')\, f_3(\beta) \tag{13}$$

$$f_1(\bar{\varepsilon}_1) = \frac{1}{\sqrt{1+250\bar{\varepsilon}_1}} \tag{14}$$

$$f_2(f_c') = \frac{69.9}{\sqrt{f_c'}} \leq 0.9 \ (f_c' \text{ and } \sqrt{f_c'} \text{ in psi}), \tag{15}$$

$$f_3(\beta) = 1 - \frac{|\beta|}{24°}. \tag{16}$$

One of the main outcomes of this study was to develop a fourth function that can account for the presence of FRP sheets on the RC panels. As discussed in this study the presence of FRP sheets increased the softening coefficient as expected due to the additional confinement effect and the different crack pattern. This increase ranged from 6.5 to 21% depending on the smeared tensile strains and thickness of the FRP sheets.

This function should be furnished so that it can reflect the material properties (modulus of elasticity), thickness and other contributions that FRP sheets bring to the structure.

In summary, the softening relationship should be maintained as:

$$\zeta = f_1(\bar{\varepsilon}_1)\, f_2(f_c')\, f_3(\beta)\, f_4(FRP) \qquad (17)$$

Using a least squared error fit, the following expression was found to best fit the effect of FRP sheets on the softening coefficient relationship:

$$f_4(FRP) = (1 + E_{FRP}/10^6 \times \bar{\varepsilon}_1^{-1.05} \times (\frac{t_{FRP}}{0.011})^{\left(\frac{2}{3}\right)})(1.12 - 16 \times \bar{\varepsilon}_1) \qquad (18)$$

This function equals 1 when FRP is not present.

This function results in the 2 curves shown in Figure 13 which closely correlate with the experimental test data. For further simplification, the following expression was recommended for ease of practice using psi for modulus of elasticity and inches for thickness of FRP:

$$f_4(FRP) = (1 + \frac{E_{FRP} \times \bar{\varepsilon}_1 \times t_{FRP}^{\left(\frac{2}{3}\right)}}{50,000})(1.12 - 16 \times \bar{\varepsilon}_1) \qquad (19)$$

SUMMARY AND CONCLUSION

This paper aims at developing new constitutive relations for RC elements strengthened with FRP sheets. To accomplish this goal, a series of representative specimens were tested using the Universal Panel Tester at the University of Houston under sequential shear loading. Several successfully performed tests were presented in this study, and different data were extracted from the experimental results to allow developing the new constitutive relations. Finally, a new stress softening coefficient was derived. Depending on the tensile strain, a range of 6.5 to 21% increase in the stress softening coefficient can be observed due to the effect of the FRP strips. The new relationships can be readily used in finite element models to properly define the material constitutive behavior and better predict the structural performance of concrete members retrofitted with FRP sheets. The constitutive model will be improved with additional data points

resulting from new experiments that will address the different parameters that can influence the behavior.

ACKNOWLEDGEMENTS

REFERENCES

ACI 440-02, Guide for the Design and Construction of Externally Bonded FRP Systems for Strengthening Concrete Structures, American Concrete Institute, Farmington Hills, MI, 2002.

Belarbi, A., and Hsu, T. T. C., 1994, "Constitutive Laws of Concrete in Tension and Reinforcing Bars Stiffened by Concrete," ACI Structural Journal, V. 91, No. 4, pp. 465-474.

Belarbi, A., and Hsu, T. T. C., 1995, "Constitutive Laws of Softened Concrete in Biaxial Tension-Compression," ACI Structural Journal, V. 92, No. 5, pp. 562-573.

Cao, S. Y., Chen, J. F., Teng, J. G., Hao, Z., and Chen, J., 2005, "Debonding in RC Beams Shear Strengthened with Complete FRP Wraps," Journal of Composites for Construction. Vol. 9, No. 6, pp. 488-496.

Carolin, A., and Taljsten, B., 2005, "Theoretical Study of Strengthening for Increasing Shear Capacity," Journal of Composites for Construction. Vol. 9, No. 6, pp. 497-506.

Chaallal, O., Nollet, M.J., and Perraton, D., 1998, "Shear Strengthening of RC Beams by Externally Bonded Side CFRP Strips," Journal of Composites for Construction, Vol. 2, No. 2, pp. 111-114.

Chaallal, O., Shahawy, M., and Hassan, M., 2002, "Performance of Reinforced Concrete T-Girders Strengthened in Shear with Carbon Fiber-Reinforced Polymer Fabric," ACI Structural Journal, Vol. 99, No. 3, pp. 335-343.

Chen, J. F., and Teng, J.G., 2003a, "Shear Capacity of FRP Strengthened RC Beams: FRP Debonding," Construction Building Materials, Vol. 17, No. 1, pp. 27-41.

Chen, J. F., and Teng, J.G., 2003b, "Shear Capacity of FRP Strengthened RC Beams: FRP Rupture," Journal of Structural Engineering, Vol. 129, No. 5, pp. 615-625.

Deniaud, C., and Cheng, J. J. R., 2004, "Simplified Shear Design Method for Concrete Beams Strengthened with Fiber Reinforced Polymer Sheets," Journal of Composites for Construction, Vol. 8, N0.5, pp. 425-433.

Hoffman, N., 2010, Constitutive Models of Prestressed Steel-Fiber Concrete, Department of Civil and Environmental Engineering, University of Houston, Houston, TX.

Hsu, T. T. C.; Belarbi, A.; and Pang. X. B., 1995, "Universal Panel Tester," Journal of Testing and Evaluations, ASTM, V. 23, No. 1, pp. 41-49.

Hsu, C. T. T., Punurai, W., and Zhang., 2003, "Flexural and Shear Strengthening of RC Beams Using Carbon Fiber Reinforced Polymer Laminates," SP-211-05, Large Scale Structural Testing, pp. 89-114.

Khalifa, A., Gold, W.J., Nanni, A., and Aziz, A.M.I., 1998, "Contribution of Externally Bonded FRP to Shear Capacity of RC Flexural Members," Journal of Composites for Construction, Vol. 2, No. 4, pp. 195-202.

Khalifa, A., 1999, Shear Performance of Reinforced Concrete Beams Strengthened with Advanced Composites, Ph.D. thesis, Department of Structural engineering, University of Alexandria, Egypt.

Laskar, A., Wang, J., Hsu, T.T.C and Mo, Y.L., "Cyclic Softened Membrane Model for Prestressed Concrete," Proceeding of ASCE Structures Congress 2008.

Lu, F., and Ayoub, A.S., 2011, "Evaluation of debonding failure of reinforced concrete girders strengthened with FRP laminates", Journal of Construction and Building Materials, Vol. 25, No. 4, pp. 1963-1979.

Monti, G., and Liotta, M.A., 2005, "FRP-Strengthening in Shear: Tests and Design Equation,"

SP-230-32, ACI Proceedings of the 7th International Symposium on FRP for Reinforcement of Concrete Structures (FRPRCS-7). pp. 543-562.

Mullapudi, T.R. and Ayoub, A.S. "Modeling the seismic behavior of shear-critical reinforced concrete columns", Journal of Engineering Structures, 32 (11): 3601–3615, (2010).

Pang, X. B., and Hsu, T. T. C., 1995, "Behavior of Reinforced Concrete Membrane Elements in Shear," ACI Structural Journal, V. 92, No. 6, pp. 665-679.

Pellegrino, C., and Modena, C., 2002, "Fiber Reinforced Polymer Shear Strengthening of Reinforced Concrete Beams with Transverse Steel Reinforcement," Journal of Composites for Construction, Vol. 6, No. 2, pp. 104-111.

Triantafillou, T. C., 1998, "Shear Strengthening of Reinforced Concrete beams Using Epoxy-Bonded FRP Composites," *ACI Structural Journal*, Vol. 95, No. 2, pp. 107-115.

Triantafillou, T.C., and Antonopoulos, C. P., 2000, "Design of Concrete Flexural Members Strengthened in Shear with FRP," Journal of Composites for Construction, Vol. 4, No. 4, pp. 198-205.

Tumialan, R. P., 2007, Performance Evaluation of Existing Analytical Methods to Compute the Shear Contribution Provided by Externally Bonded FRP Sheets in Concrete Structures, Department of Civil, Environmental and Architectural Engineering, Missouri University of Science and Technology, Rolla, Mo.

Wang, T. J. and Hsu, T. T. C., 2001, "Nonlinear Finite Element Analysis of Concrete Structures Using New Constitutive Models," Computers and Structures, Vol. 79, No. 32, Dec. 2001, pp. 2781-2791.

Zhang, L. X., and Hsu, T. T. C., 1998, "Behavior and Analysis of 100 MPa Concrete Membrane

Elements," ASCE Journal of Structural Engineering, V. 124, No. 1, pp. 24-34.

Zhang, Z., and Hsu, C.T.T., 2005, "Shear Strengthening of Reinforced Concrete Beams Using Carbon-Fiber-Reinforced polymer Laminates," Journal of Composites for Construction, Vol.1, pp. 491-498.

Table 1 -- Rebar Configuration and FRP Wrapping Scheme

Panel name	Rebar Configuration	FRP Wrapping Scheme
F1P-1	A	A
F1P-2	A	B
F1P-3	B	C
F1P-4	B	C
F1P-5	B	C
F1P-6	B	C
F1P-7	B	C
F1P-8	A	C
F2P-1	A	C
F2P-2	B	C
F2P-3	B	C
F2P-4	B	C

Table 2 -- Details and Parameters of Panels F1P and F2P

Specimen	ρ_ℓ	ρ_t	$f'_{c,}$ ksi (MPa)	$\bar{\varepsilon}_\ell$
F1P-3	0.52%	0.52%	5.79 (39.9)	0.5%
F1P-5	0.52%	0.52%	6.65 (45.8)	0.75%
F1P-7	0.52%	0.52%	6.05 (41.7)	0.3%
F1P-8	0.52%	0.52%	4.03 (27.8)	0.0%
F2P-1	0.52%	0.52%	5.08 (35.0)	0.0%
F2P-2	0.52%	0.52%	5.61 (38.6)	0.75%
F2P-3	0.52%	0.52%	6.06 (41.7)	0.5%
F2P-4	0.52%	0.52%	4.79 (33.0)	0.3%

Table 3 -- Compressive Peaks and Stress Softening Coefficients

Panel	ε_ℓ (in./in.)	$f_c^{'}$ ksi (MPa)	σ_c ksi (MPa)	ζ_σ ksi/ksi (MPa/MPa)	ζ_σ Predicted RC ksi/ksi (MPa/MPa)	Percent Difference (%)
F1P-3	0.005	5.79 (39.9)	3.71 (25.6)	0.64	0.66	3
F1P-5	0.0075	6.65 (45.8)	3.89 (26.8)	0.58	0.58	0
F1P-7	0.003	6.05 (41.7)	4.63 (31.9)	0.77	0.75	2.7
F1P-8	0	4.03 (27.8)	4.19 (28.9)	1.04	1.00	4
F2P-1	0	5.08 (35.0)	5.08 (35.0)	1.00	1.00	0
F2P-2	0.007	5.61 (38.6)	3.70 (25.5)	0.66	0.64	3.1
F2P-3	0.005	6.06 (41.7)	4.06 (28.0)	0.67	0.70	4.3
F2P-4	0.003	4.79 (33.0)	3.64 (25.1)	0.76	0.78	2.6

Figure 1 -- Universal Panel Tester North Side

Figure 2 -- Universal Panel Tester South Side

Rebar Configuration A   Rebar Configuration B
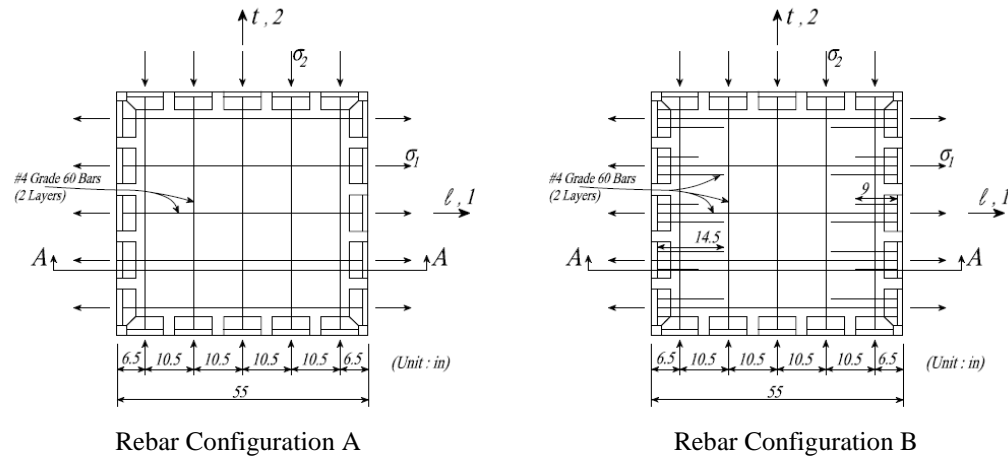
Figure 3 – Reinforcement Details

Wrapping Configuration A   Wrapping Configuration B   Wrapping Configuration C
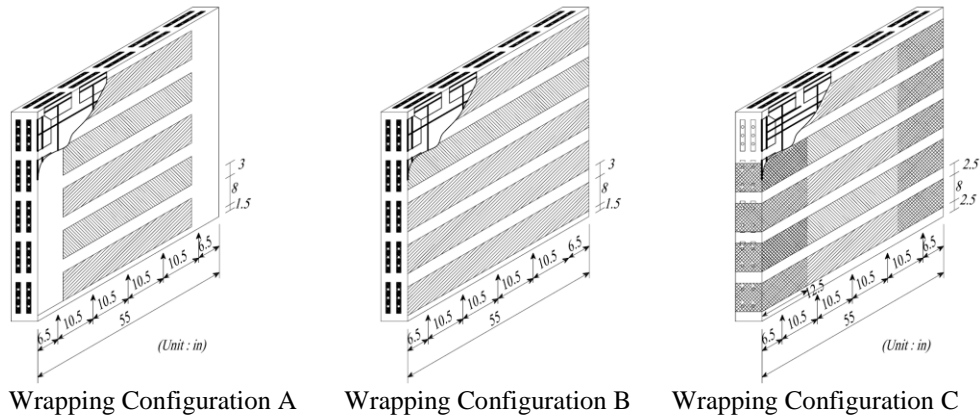
Figure 4 – FRP Wrapping Schemes

Specimen	South Side	North Side
F1P-3		
F1P-5		
F2P-2		

Figure 5 – Crack Pattern for Specimens at Target Tensile Strains
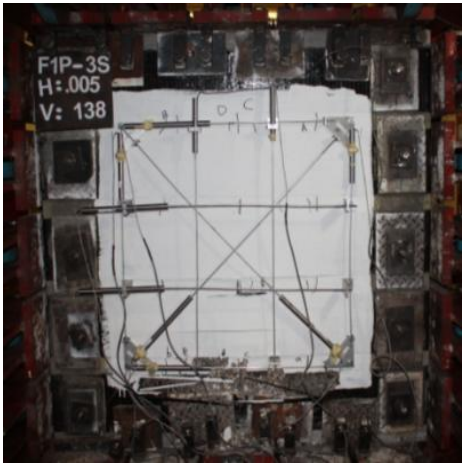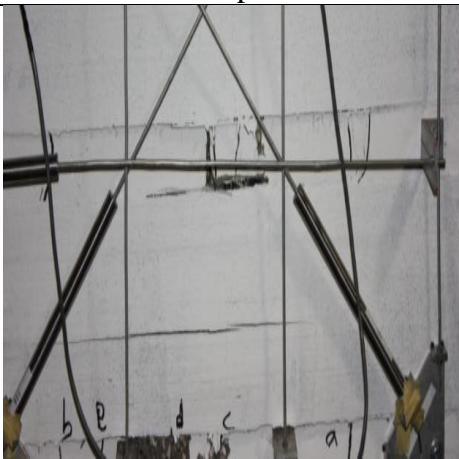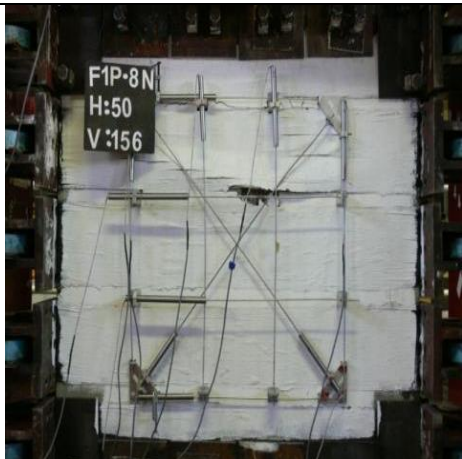
Specimen	Panel View	Close-up View
F1P-3		
F1P-8		
F2P-3		

Figure 6 – Crushing of Specimens at Failure
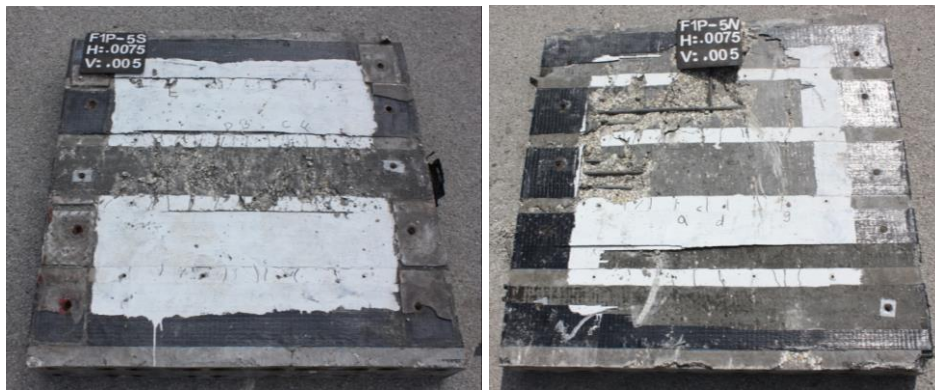
Figure 7 -- Panel F1P-5 at Failure

Figure 8 -- Panel F2P-2 at Failure
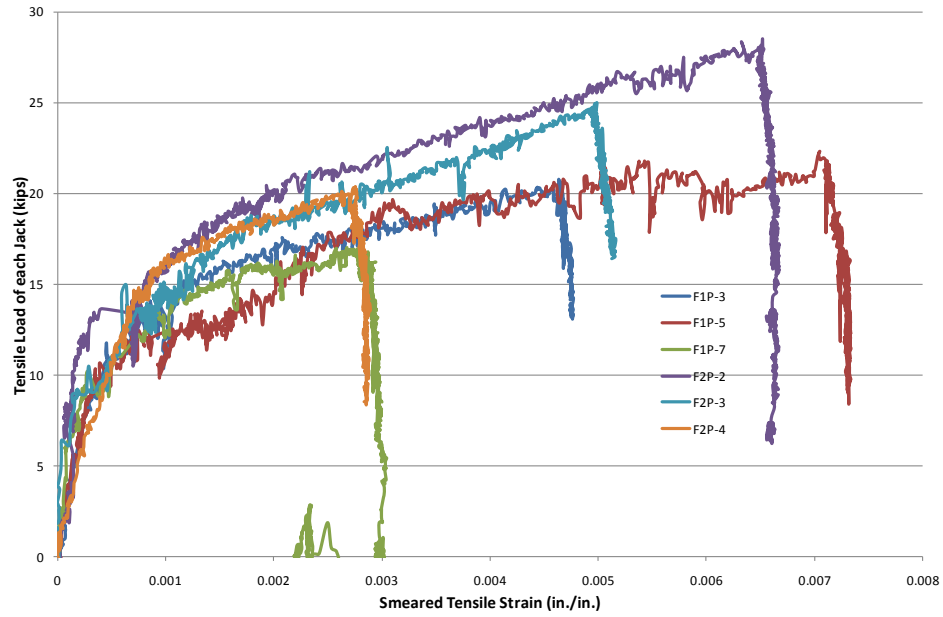
Figure 9 –Smeared Stress-Strain Curve in Tension for Specimens
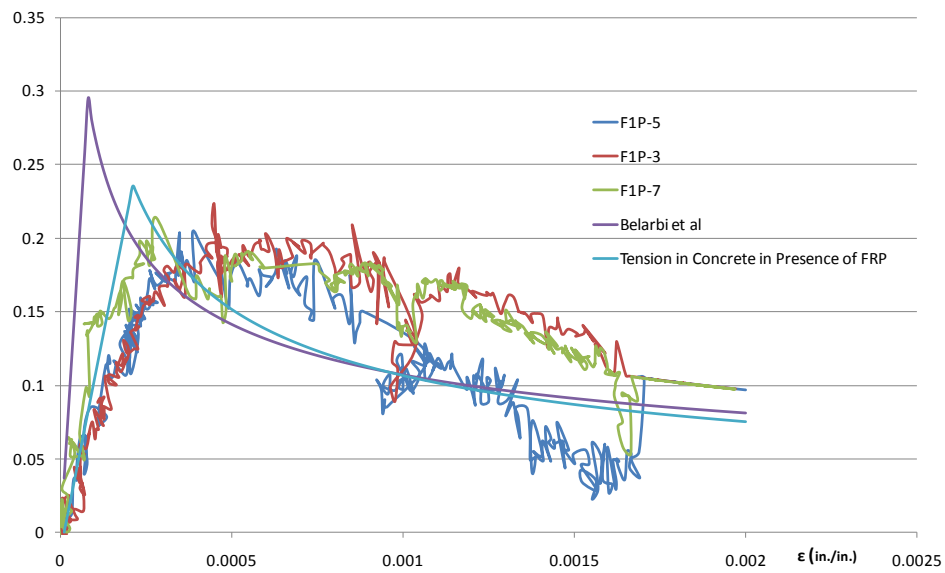
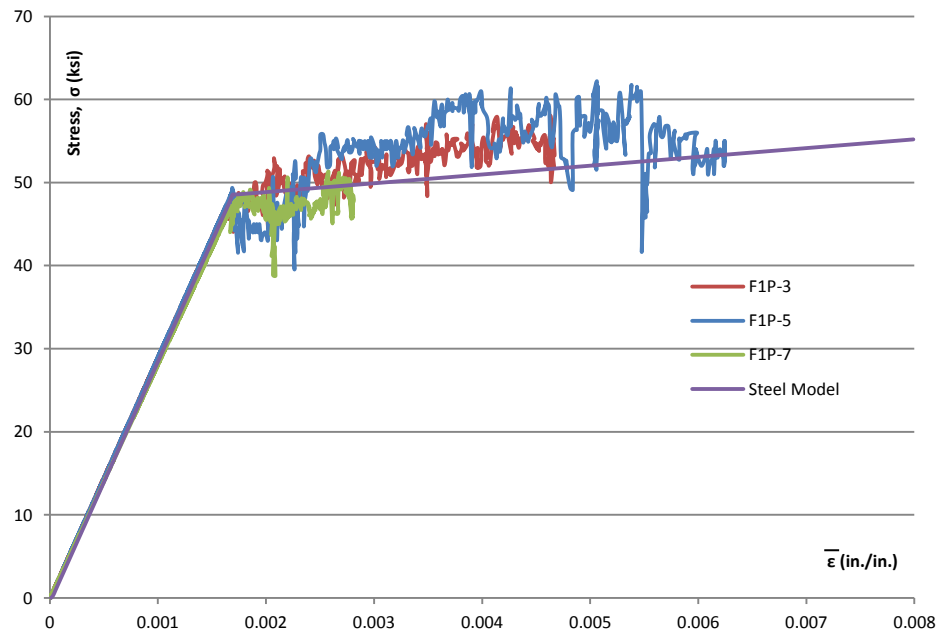**Figure 10 – Stress-Strain Curve of Concrete in Tension for F1P Specimens**

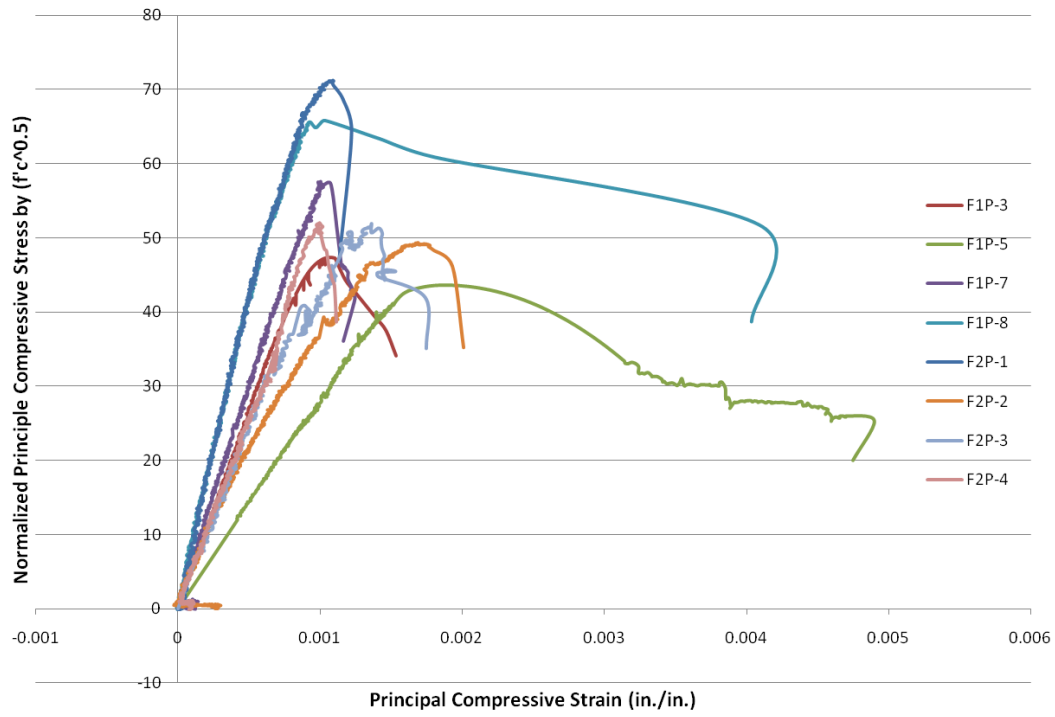**Figure 11 - Stress-Strain Curve of Embedded Steel in Tension for F1P Specimens**

Figure 12 – Normalized Stress-Strain Curve of Concrete in Compression for all Specimens
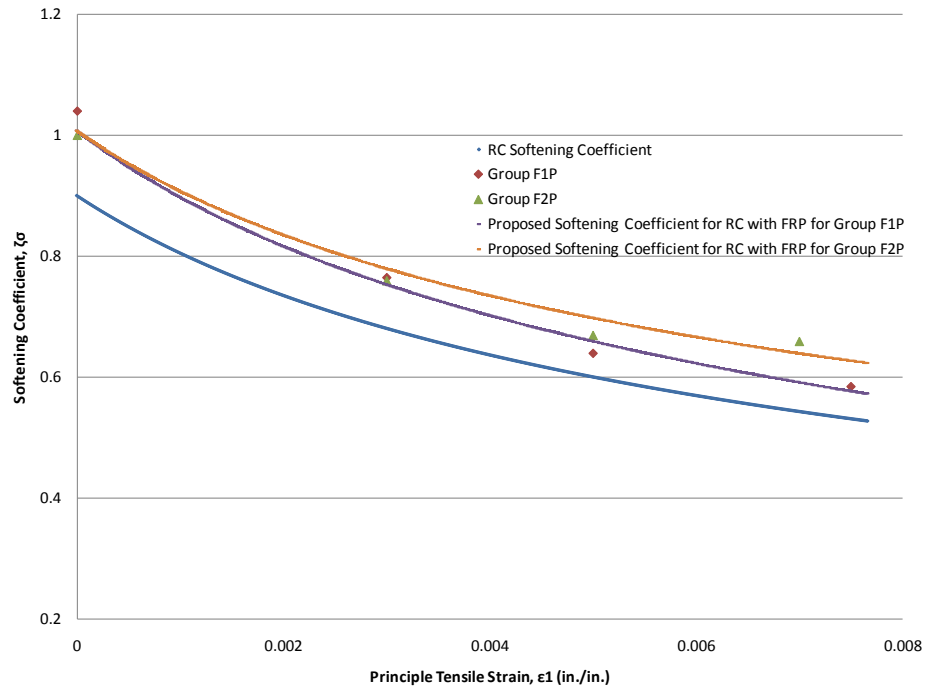
Figure 13 – Peak Stress Softening Coefficient Curve for RC elements strengthened with FRP Sheets